Compatibilizer-Tracer: A Powerful Concept for Polymer-Blending Processes

Cai-Liang Zhang
State Key Laboratory of Chemical Engineering, Dept. of Chemical and Biochemical Engineering, Zhejiang University, Hangzhou 310027, China

Laboratory of Reactions and Process Engineering, Nancy University, CNRS-ENSIC-INPL, 1 rue Grandville, BP 20451, 54001 Nancy, France

Lian-Fang Feng
State Key Laboratory of Chemical Engineering, Dept. of Chemical and Biochemical Engineering, Zhejiang University, Hangzhou 310027, China

Sandrine Hoppe
Laboratory of Reactions and Process Engineering, Nancy University, CNRS-ENSIC-INPL, 1 rue Grandville, BP 20451, 54001 Nancy, France

Guo-Hua Hu
Laboratory of Reactions and Process Engineering, Nancy University, CNRS-ENSIC-INPL, 1 rue Grandville, BP 20451, 54001 Nancy, France

Institut Universitaire de France, Maison des Universités, 103 Boulevard Saint-Michel, 75005 Paris, France

DOI 10.1002/aic.12723
Published online July 27, 2011 in Wiley Online Library (wileyonlinelibrary.com).

Polymer blending is a very important polymer processing operation. It aims at preparing new polymer materials by blending existing polymers without the need of creating new molecules. For immiscible polymer blends, it is always challenging, if not impossible, to choose an appropriate compatibilizer and assess its compatibilizing efficiency under pilot or industrial polymer-blending conditions. The concept of compatibilizer-tracer developed in this work is able to take this challenge. This is shown using polystyrene (PS)/polyamide 6 (PA6) blends and fluorescent labeled graft copolymers of PS and PA6 as compatibilizer-tracer. Transient experiments allow using very small amounts of compatibilizer-tracer to obtain emulsification curves, namely, the evolution of the dispersed phase domain size as a function of the compatibilizer-tracer concentration. Other potential applications of this concept are discussed and its limitations are investigated. © 2011 American Institute of Chemical Engineers *AIChE J,* 58: 1921–1928, 2012
Keywords: compatibilizer-tracer, polymer blend, emulsification curve, in-line measurement, twin-screw extruder

Introduction

Blending existing polymers is a very attractive and inexpensive way of obtaining new materials without the need to create new molecules.[1,2] Polymer-blending processes use mainly batch mixers and continuous mixers of type screw extruder, especially twin-screw extruder. The former are mainly used in the laboratory and the latter both in the laboratory and for industrial production.

As most polymers are mutually immiscible, a compatibilizer of type block or graft copolymer is often required. A so-called emulsification curve, which essentially follows the evolution of the dispersed phase domain size of a polymer blend as a function of the compatibilizer concentration, is successfully used to evaluate the interfacial behavior and efficiency of the compatibilizer.[2–8] When a batch mixer is used, the emulsification curve can be built up in the following manner. Given compositions of the polymer components of the blend as well as the copolymer are charged to the mixer. After a certain elapse of time (usually 5–10 min), the process reaches a steady state and samples are taken from the mixer. The size of the dispersed phase domains of the blend is measured. This makes up a point on the emulsification curve. The above process is repeated upon varying the copolymer concentration. An emulsification curve is then built up for the said composition of the blend. In the case of a screw extruder, the so-called steady-state experiments can also be carried out. They are similar to those in a batch mixer. Given compositions of the polymer components of the blend as well as the copolymer are charged to the hopper of the extruder. After a certain elapse of time (usually more than 10 times the average residence time), the process reaches a steady state and samples are taken from the die exit for measurement.

Correspondence concerning this article should be addressed to L.-F. Feng at fenglf@zju.edu.cn and G.-H. Hu at guo-hua.hu@ensic.inpl-nancy.fr.

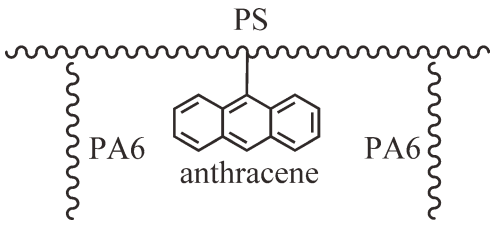

Figure 1. Schematic of the structure of PS-g-PA6-Ant compatibilizer-tracer.

Studies reported in the literature concerning emulsification curves often use batch mixers and not screw extruders. The main reason is that batch mixers are often more accessible in a laboratory than twin-screw extruders and that they are much easier to operate too. More importantly, the amount of the copolymer required for building up an emulsification curve in a batch mixer is often much smaller than in a twin-screw extruder. This is especially true for a pilot or industrial-scale screw extruder of which the production rate can reach from a few dozens of kilograms per hour to a few tones per hour. In such a case, the amount of the copolymer required may be too large to build up an emulsification curve.

This work aims at developing a so-called compatibilizer-tracer concept for polymer-blending processes in order that a very small amount of copolymer still allows building up an emulsification curve in a pilot or industrial-scale screw extruder. The idea is based on the transient experiments for measuring residence time distributions.[9–12] Unlike a steady-state experiment in which given compositions of the polymer components of the blend and the compatibilizer are charged to the hopper of the extruder altogether, in a transient experiment, the polymer components are first fed to the hopper of the extruder. When the process reaches its steady state, a given and small amount of the copolymer is introduced to the hopper of the extruder as a pulse. Samples are taken at the die exit as a function of time. Both the evolution of the copolymer concentration and that of the morphology as a function of time can be obtained. The former provides the compatibilizer concentration distribution (CCD) and the latter the dispersed phase domain size distribution (DSD) for dispersed type polymer blends. From both distributions, the emulsification curve should easily be deduced.

The usefulness of the compatibilizer-tracer concept for building emulsification curves under real polymer-blending conditions and with a small amount of compatibilizer-tracer is shown using the blends composed of polystyrene (PS) and polyamide 6 (PA6). The corresponding compatibilizer-tracer is a graft copolymer with PS as a backbone and PA6 as grafts. It also contains anthracene moieties along the PS backbone as shown in Figure 1 and is designated as PS-g-PA6-Ant.[13] Other potential applications including process optimization and limitations are discussed.

Table 1. Selected Characteristics of the PS and PA6 Used in This Work

	Number average molar mass (M_n)*	Weight average molar mass (M_w)*	Supplier
PS	101.3 kg/mol	228.8 kg/mol	Yangzi-BASF Styrenics Co., Nanjing, China
PA6	19.4 kg/mol	49.4 kg/mol	UBE Nylon Ltd., Thailand

*Molar masses measured by size exclusion chromatography (SEC) using PS standards for the calibration and THF as the eluent. The PA6 was first *N*-trifluoroacetylated before the SEC measurement. A ultraviolet (UV) detector at 238 nm was used for the SEC measurement.

Table 2. Molar Masses, PA6, and 9-(methylamino-methyl)anthracene (MAMA) Contents of the Compatibilizer-Tracers

Sample	M_n[a] (kg/mol)	M_w[a] (kg/mol)	PA6 content[b] (wt%)	MAMA content[c] (wt%)
PS-g-PA6-Ant1	37.8	137.0	35.3	0.10
PS-g-PA6-Ant2	32.3	88.2	13.2	0.23

[a]Molar masses of *N*-trifluoroacetylated PS-g-PA6 by SEC using a refractometer (RI) detector and based on the PS standards.
[b]SEC using dual UV detection at 238 and 260 nm.
[c]UV at 367 nm.

Experimental

Materials

The PS and PA6 used were in the form of pellets of about 2–4 mm in diameter. The PS-g-PA6-Ant compatibilizer-tracer was synthesized and characterized in the laboratory following the procedures reported in the literature.[14–16] Table 1 gathers the selected characteristics of the PS and PA6 and Table 2 those of two PS-g-PA6-Ant graft copolymers. The main difference between those two graft copolymers lies in the fact that the both the content and length of PA6 grafts in PS-g-PA6-Ant1 were much more important than those in PS-g-PA6-Ant2.

The rheological behavior of the pure polymer components and their blends was characterized by an advanced rheometric expansion system of type TA Instrument, USA. A dynamic mode was used to measure the complex viscosity (η^*) as a function of frequency. The samples were disks of 25 mm in diameter and about 2 mm in thickness. The strain amplitude was set at 10%, which was in the range of the linear viscoelastic shear oscillation. Figure 2 shows the complex viscosity at 230 °C of the PS, PA6, and their blends with mass compositions of 80/20 and 18.5/81.5 as a function of frequency. At low frequency, the complex viscosity of the PA6 was lower than that of the PS. The two PS/PA6 blends were in between the PS and PA6, as expected. Moreover,

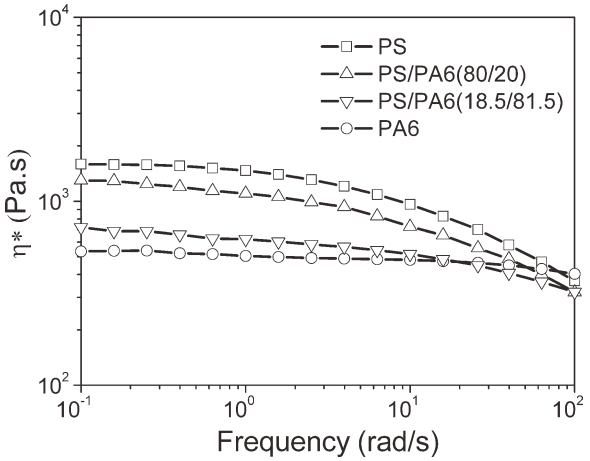

Figure 2. Complex viscosity vs. frequency for the PS, PA6, and PS/PA6 (80/20 and 18.5/81.5 by mass) blends at 230 °C.

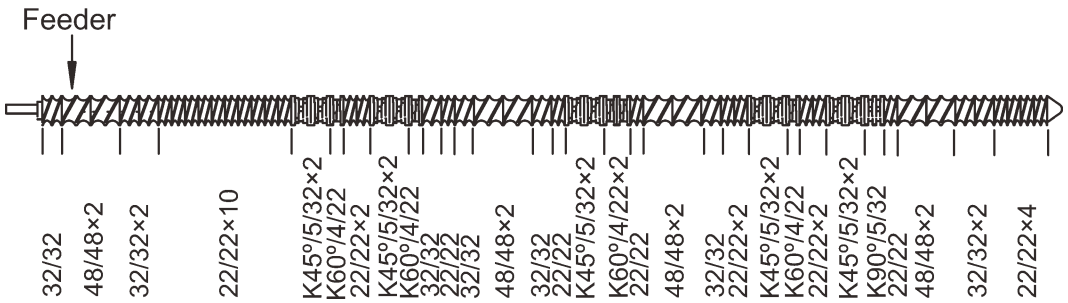

Figure 3. Screw configuration of the twin-screw extruder.

the viscosity of the PS/PA6 (18.5/81.5 by mass) blend was lower than that of the PS/PA6 (80/20 by mass). At high frequency, the complex viscosities of the PS, PA6, and their blends became closer.

Polymer-blending process and in-line compatibilizer-tracer concentration measurement

The polymer-blending process was carried out on a corotating twin-screw extruder with a diameter of 35 mm and a length to diameter ratio of 48 from Nanjing Ruiya Extrusion System Limited, China. Figure 3 shows the screw configuration. Basically, it was consisted of right-handed screw elements and kneading blocks. The head of the extruder was equipped with a strip die, as shown in Figure 4.

The barrel temperature and screw speed were set at 230°C and 100 rpm, respectively. The feed rate of the PS/PA6 blend to the extruder was 13 kg/h. Under those conditions, the overall average degree of fill in the extruder was about 50% with the kneading disks and strip die fully filled and the conveying zones partially filled. The PS/PA6 blend composition was 90/10, 80/20, or 18.5/81.5 by mass. When the extruder ran steadily, a given amount (a few grams maximum) of a PS-g-PA6-Ant compatibilizer-tracer was added to it from the hopper as a pulse. At the same time, the fluorescent signal started recording at the extruder die exit using an in-line residence time distribution measurement device developed previously.[17–20] Before the signal started increasing, a sample of the extrudate was taken from the die and was used as a reference. Subsequently, samples were taken once every 10 seconds till the signal reached its baseline value. They were quenched immediately in liquid nitrogen to freeze-in their morphologies.

Unless specified otherwise, the compatibilizer-tracer and the die width were PS-g-PA6-Ant1 and 5 mm, respectively.

With the assumption that the compatibilizer-tracer concentration was proportional to the analog fluorescent signal in voltage, the normalized CCD (also residence time distribution) function could be calculated according to the following expression:

$$E(t_i) = \frac{V_i(t)}{\sum_{i=1}^{n} V(t_i)(t_i - t_{i-1})} \tag{1}$$

where V_i is the voltage at time t_i ($i = 1, 2, \ldots, n$).

Morphology characterization

The morphology of the blends was characterized using a scanning electron microscopy (SEM) of JEOL Model JSM-330A instrument. Before the SEM observations, samples were first fractured in liquid nitrogen. The fractured surfaces were then immersed in formic acid to remove the PA6 dispersed phase from the PS/PA6 (90/10 and 80/20 by mass) blends or in tetrahydrofuran (THF) to remove the PS dispersed phase from the PS/PA6 (18.5/81.5 by mass) blends at room temperature for 12 h. They were dried for 12 h in a vacuum oven at 80 °C and then gold sputtered. The voltage for the SEM was 5.0 kV.

The diameter of the dispersed phase domains was measured using a semiautomatic image analysis method. It was characterized by volume average particle diameters, d_v, defined by:

$$d_v = \frac{\sum n_i d_i^4}{\sum n_i d_i^3} \tag{2}$$

For each blend, at least 500 particles were counted for statistically meaningful values of d_v.

Results

Figure 5 shows the CCD and DSD curves for the PS/PA6 blends with PS-g-PA6-Ant1 (1.6 g) as the compatibilizer-tracer. Their PS/PA6 compositions were 90/10, 80/20 and 18.5/81.5 by mass, respectively. In the two former, the PS was the matrix and the PA6 the dispersed phase, whereas, in the latter, the matrix and the dispersed phase were reversed. The matrix/dispersed phase volume ratios of the last two compositions were the same. For a given amount of compatibilizer-tracer added to the extruder as a pulse, a minimum elapse of time was necessary before it exited from the die. The two CCD curves for the PS/PA6 (90/10 and 80/20 by mass) blends almost superimpose, as expected. The minimum elapse of time for the PS/PA6 (18.5/81.5 by mass) blend was shorter. Moreover, after the minimum elapse of time, the compatibilizer-tracer mass fraction starts increasing

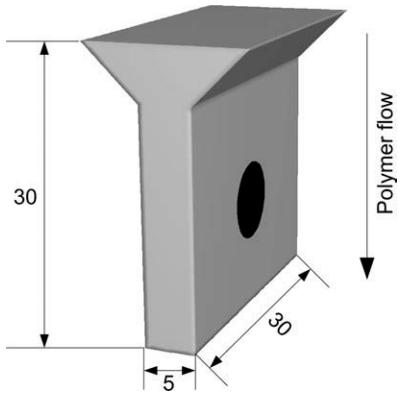

Figure 4. Geometry of the strip die.

The black dot is the location of the fluorescent probe.

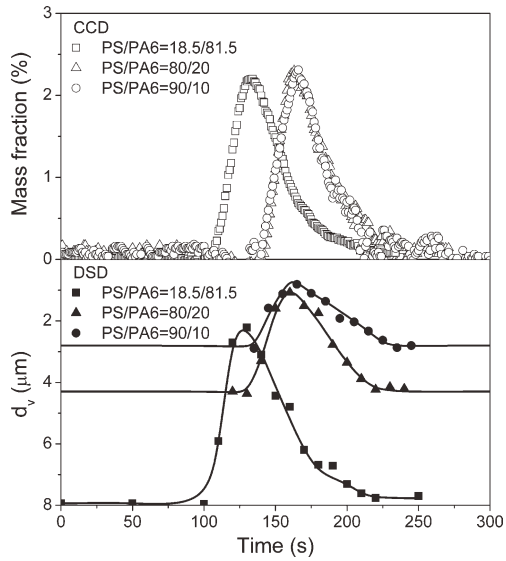

Figure 5. CCD and DSD of the PS/PA6 blends for three different PS/PA6 compositions with PS-g-PA6-Ant1 as the compatibilizer-tracer.

Feed rate: 13 kg/h; pulse of the compatibilizer-tracer: 1.6 g; screw speed: 100 rpm.

with time till a maximum is reached. Thereafter, it starts decreasing with a further increase in time. After a sufficiently long period of time, all the initial amount of the compatibilizer-tracer is washed out and the compatibilizer-tracer mass fraction becomes zero again.

Concomitantly, the dispersed phase domain size follows the opposite trend. This is because the higher the compatibilizer-tracer concentration in the extrudate, the smaller the dispersed phase domain size. More interestingly, the dispersed phase domain size of the PS/PA6 blend follows the order: PS/PA6 (90/10 by mass) < PS/PA6 (80/20 by mass) < PS/PA6 (18.5/81.5 by mass). In the first two blends, the PS is the matrix and the PA6 is the dispersed phase. The fact that the domain size of the PS/PA6 (80/20 by mass) blend is higher than that of the PS/PA6 (90/10 by mass) indicates that it is more difficult for the compatibilizer to prevent the dispersed phase domains from coalescence when the dispersed phase fraction is higher. The PS/PA6 (18.5/81.5 by mass) and PS/PA6 (80/20 by mass) blends have the same matrix/dispersed phase volume ratio, except that the matrix and dispersed phase are reversed. The dispersed phase size of the former is much bigger than that of the latter, indicating that the compatibilizing efficiency of the PS-g-PA6-Ant for the former is much lower than that in the latter. This is in line with a conclusion drawn in the literature[8] that it is better to choose a graft copolymer with the matrix polymer as the backbone and the dispersed phase polymer as grafts.

The emulsification curves can easily be deduced from both the CCD and DSD ones in Figure 5, as shown in Figure 6. Three interesting remarks can be made. Firstly, for all the three PS/PA6 blends, the dispersed phase domain size decreases with increasing compatibilizer-tracer concentration, as expected from classical steady-state experiments. Secondly, the emulsification curve of the PS/PA6 (18.5/81.5 by mass) blend is located well above that of the PS/PA6 (80/20 by mass). The latter is above that of the PS/PA6 (90/10 by mass) blend. This further confirms the above statement that the compatibilizing efficiency of the PS-g-PA6-Ant whose backbone is PS is higher for PS/PA6 blends whose matrix is PS than for those whose matrix is PA6. Thirdly, each of the emulsification curves is not a single curve but a loop. These emulsification loops are obtained in the following manner. A CCD curve is divided into short and long time domains which are demarcated by its maximum. In the short time domain, the compatibilizer-tracer fraction increases with the increasing residence time, whereas, in the long time domain, it follows the opposite trend. When the dispersed phase domain size is plotted against the compatibilizer concentration, two curves are generated. Moreover, for all the three PS/PA6 blends, whether the PS is the matrix or dispersed phase, their emulsification curves in the long time domain are always located above the corresponding ones in the short time domain.

Discussion

Physical meanings of the emulsification loops

The above results show that the compatibilizer-tracer concept allows building up the emulsification curves under real polymer-blending conditions with a small amount of a compatibilizer-tracer. However, the emulsification curves are not single ones but loops. Moreover, those in the long time domain are located above the corresponding ones in the short time domain. Why? What do these results mean?

Does the fact that the emulsification curves in the long time domain are located above the corresponding ones in the short time domain mean that the graft copolymer used loses, to some extent, its compatibilizing efficiency in the long time domain? If so, could it mean that, during the blending process, shear may pull graft copolymer chains off the interfaces?[21–23] This phenomenon is expected to be more severe in the long time domain than that in the short time domain. The fact that the emulsification curves in the long time domain are located above the corresponding ones in the short time domain could also be related to coalescence between dispersed phase domains. It is expected to be more severe in the long time domain too[23] and can be accelerated by shear-induced pull-off of the graft copolymer chains. Although the above arguments seem to be convincing, there are no experimental evidences to support them.

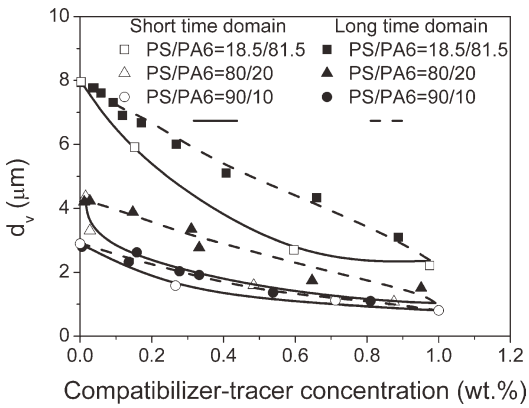

Figure 6. Emulsification curves of the PS/PA6 blends for three different PS/PA6 compositions with PS-g-PA6-Ant1 as the compatibilizer-tracer.

Feed rate: 13 kg/h; pulse of the compatibilizer-tracer: 1.6 g; screw speed: 100 rpm.

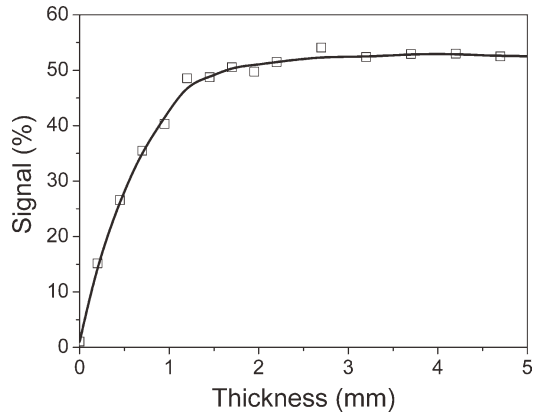

Figure 7. Relationship between the fluorescent signal and the thickness of PS/PA6/PS-g-PA6-Ant1 (80/20/1 by mass) blend at 230 °C.

A third argument could be related to the assumption that the compatibilizer-tracer concentration is proportional to the analog fluorescence signal. This assumption is used to calculate the CCD and might be inappropriate under the polymer-blending conditions as there is a detectable thickness associated with a fluorescent probe. This will be discussed in the following section.

Detectable thickness by the fluorescent probe

To assess the detectable thickness of PS/PA6/PS-g-PA6-Ant blends in the molten state, a device whose geometry is similar to that of the strip die is used. Its channel width can be adjusted from 15 to 0 mm through a bolt. Before the fluorescent signal recording, the channel width is kept at its maximum and the device is heated to and maintained at 230 °C. The PS/PA6/PS-g-PA6-Ant1 (80/20/1 by mass) blend in the molten state is fed to the channel. When the temperature is stabilized, the fluorescent signal is recorded at different channel widths by tightening the bolt. Figure 7 shows the relationship between the fluorescent signal and the channel width. The fluorescence signal first increases with an increasing thickness of the polymer blend and starts leveling off when the thickness reaches about 1.5 mm. This indicates that the maximum detectable thickness of the polymer blend by the fluorescent probe is about 1.5 mm. This is far below the thickness of the strip die used in this work (see Figure 4).

If there is no concentration gradient of the compatibilizer-tracer of the polymer blend in the direction perpendicular to the flow direction, the fluorescent signal should be proportional to the compatibilizer-tracer concentration, despite the fact that the maximum detectable thickness of the polymer blend by the fluorescent probe is far below the thickness of the strip die used in this work. However, this is not the case in this work, as discussed below.

A software of Fluent is used to simulate the evolution of the concentration profile of the compatibilizer-tracer of the PS/PA6 (80/20 by mass) blend in the channel of the extruder die as a function of time. For that purpose, meshing was carried out by a commercial preprocessor software GAMBIT (Fluent Inc.). The flow was assumed to be an isothermal,

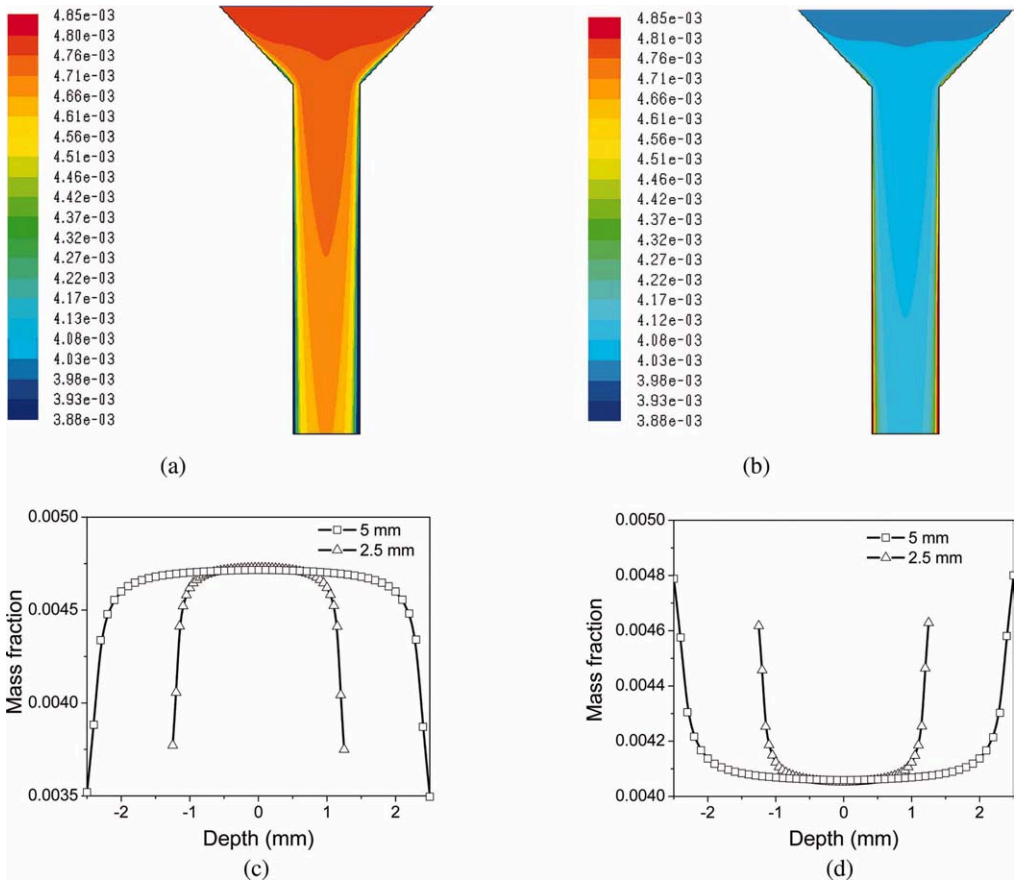

Figure 8. Concentration profiles of the PS-g-PA6-Ant1 for the PS/PA6 (80/20 by mass) blend in the 5-mm die channel (a and b) and at the florescent probe locations (c and d) for the 2.5- and 5-mm extrusion dies.

(a) and (c) 25 s; (b) and (d) 45 s. [Color figure can be viewed in the online issue, which is available at wileyonlinelibrary.com.]

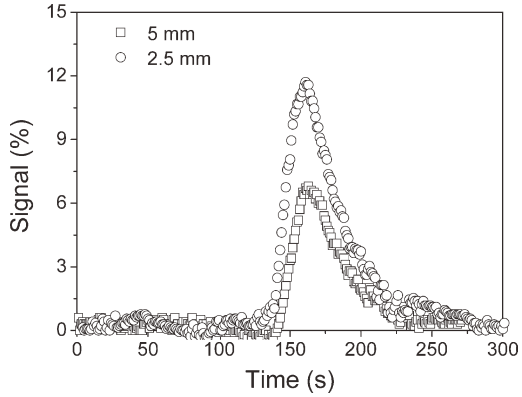

Figure 9. Comparison between two strip dies (5 and 2.5 mm in width) in terms of the evolution of fluorescent signal for PS/PA6 (80/20 by mass) blend with PS-g-PA6-Ant1 as the compatibilizer-tracer vs. the residence time.

Feed rate: 13 kg/h; mass of the compatibilizer-tracer pulse: 1.6 g; screw speed: 100 rpm.

incompressible, and generalized Newtonian fluid with no body forces. The viscosity was set at 2000 Pa s. The no-slip boundary conditions were imposed to the surfaces of strip die wall. The mass flow rate at the channel inlet was 13 kg/h. It was assumed that the concentration profile compatibilizer-tracer at the channel inlet was the same as that measured by the in-line fluorescent detector as shown in Figure 5. Moreover, the moment at which the compatibilizer-tracer arrived at the channel inlet was taken as time zero. The computational time step was set to 0.1 s. Figure 8a and b shows the concentration profiles of the compatibilizer-tracer at 25 and 45 s, respectively. The former corresponds to the short time domain where the concentration profile of the compatibilizer-tracer increases with time and the latter the long time domain where the concentration profile of the compatibilizer-tracer decreases with time. Figure 8c and d shows the concentration profiles of the compatibilizer-tracer at the fluorescent probe location for the 5-mm extrusion die and along the direction perpendicular to the polymer flow at 25 and 45 s, respectively. The case for the 2.5-mm extrusion die is also shown for comparison. From Figure 8c, at 25 s, the concentration of the compatibilizer-tracer near the channel wall is smaller than that in the channel center, whereas, at 45 s, it is the opposite (see Figure 8d). As the samples for the morphology characterization are taken from the channel center, the concentrations of the compatibilizer-tracer measured by the fluorescent probe in the short residence time domain are expected to be smaller than the real ones and those measured in the long residence time domain are expected to be higher than the real ones. This indicates that the emulsification curve corresponding to the short residence time domain should be shifted upward and that the one corresponding to the long residence time domain should be shifted downward. In other words, these two curves should have become closer or even superimpose. Therefore, the difference between the real concentration profile of the compatibilizer-tracer and that detected by the fluorescent probe is very likely responsible for the existence of emulsification loops obtained by the transient experiments in the twin-screw extruder. From Figure 8c and d, the concentrations of the compatibilizer-tracer measured by the fluorescent probe for the case of the 2.5-mm die are closer to the real ones than those for the 5-mm die. In other words, the emulsification curves corresponding to the short and long residence times are expected to become closer with decreasing die channel width. They may even superimpose when the die channel width is smaller than the critical detectable thickness for the fluorescent probe ($\sim$1.5 mm).

To further confirm the above simulation results, the width of the die channel was changed from 5 to 2.5 mm. Figure 9 compares the evolution of the fluorescent signal of the PS/PA6 blend (80/20 by mass) with time between the 2.5- and 5-mm dies using PS-g-PA6-Ant1 as the compatibilizer-tracer. As expected, the fluorescent signal is indeed higher for the 2.5-mm die than that for the 5-mm one.

Figure 10 compares the CCD and DSD curves between the 5- and 2.5-mm strip dies. The CCD curve corresponding to the 2.5-mm die is slightly shifted toward the shorter time domain compared with the 5-mm die, whereas both DSD curves almost fall on a single curve.

On the basis of the CCD and DSD curves, the corresponding emulsification curves can be deduced, as shown in Figure 11. As expected, compared with the 5-mm die, the emulsification curve for the 2.5-mm die in the short time domain is shifted upward, whereas the one in the long time domain is shifted downward. In other words, the two curves in the short and long time domains are much closer to each other for the 2.5-mm die, even if they do not fully superimpose yet. This confirms that the fluorescent detection depth is one of the main factors responsible for the existence of the loop phenomenon for the emulsification curves.

In what follows, two examples will be given to show how convenient and powerful the concept of compatibilizer-tracer can be. The first one is to assess the effect of the architecture of compatibilizer on its compatibilizing efficiency, and the second is to compare the efficiency of mixing between different types of mixers.

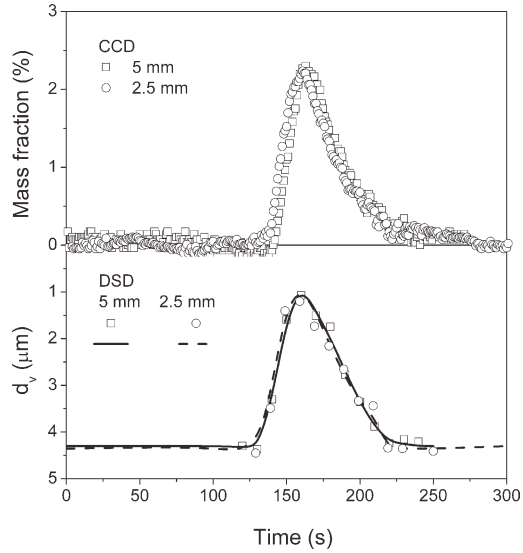

Figure 10. Effect of the strip die width on the CCD and DSD for the PS/PA6 (80/20 by mass) with PS-g-PA6-Ant1 as the compatibilizer-tracer.

Feed rate: 13 kg/h; mass of the compatibilizer-tracer pulse: 1.6 g; screw speed: 100 rpm.

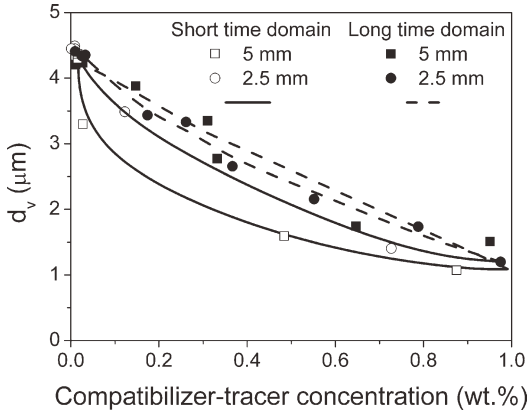

Figure 11. Effect of the extrusion die on the emulsification curve of the PS/PA6 (80/20 by mass) blend with PS-g-PA6-Ant1 as the compatibilizer-tracer.

The data are deduced from Figure 10. Feed rate: 13 kg/h; mass of PS-g-PA6-Ant1 pulse: 1.6 g; screw speed: 100 rpm.

Effect of the architecture of the compatibilizer-tracer on the emulsification curve

Figure 12 compares the CCD and DSD curves between PS-g-PA6-Ant1 and PS-g-PA6-Ant2 for the PS/PA6 (80/20 by mass) blend system. It is very interesting to note that both CCD and DSD are different for these two compatibilizer-tracers. The CCD is much narrower for PS-g-PA6-Ant1 than for PS-g-PA6-Ant2. The corresponding dispersed phase size for PS-g-PA6-Ant1 is well smaller that for PS-g-PA6-Ant2.

Figure 13 compares the compatibilizing efficiency between PS-g-PA6-Ant1 and PS-g-PA6-Ant2 in terms of the emulsification curve for the PS/PA6 (80/20 by mass) blend on the basis of the data in Figure 12. The size of the dispersed phase domains using PS-g-PA6-Ant1 as the compatibilizer-tracer is significantly lower than that for PS-g-PA6-Ant2, indicating that the compatibilizing efficiency of the former is much higher than that of the latter. PS-g-PA6-Ant1 and PS-g-PA6-Ant2 are similar in the PS backbone length and have the same number of PA6 grafts but are different in the PA6 graft length, as shown in Table 2. This

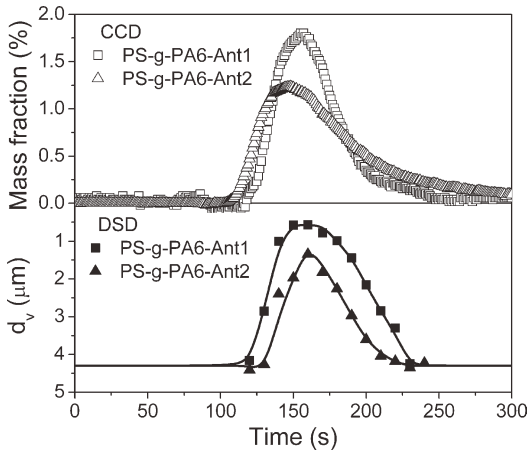

Figure 12. Comparison of the CCD and DSD curves between PS-g-PA6-Ant1 and PS-g-PA6-Ant2 for the PS/PA6 (80/20 by mass) blend system.

Die width: 5 mm; feed rate: 13 kg/mol; mass of the compatibilizer-tracer pulse: 4.8 g; screw speed: 100 rpm.

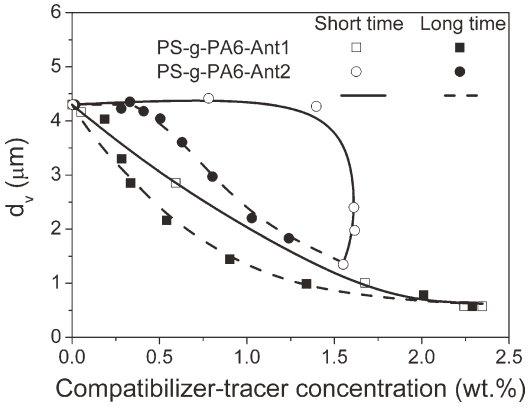

Figure 13. Effect of the molecular architecture of the compatibilizer-tracer on the emulsification curve of the PS/PA6 (80/20 by mass) blend.

Die width: 5 mm; feed rate: 13 kg/h; mass of the compatibilizer-tracer pulse: 4.8 g; screw speed: 100 rpm.

implies that a PS-g-PA6-Ant with longer grafts has higher compatibilizing efficiency. This is in line with the conclusions drawn in the literature.[7,8,24]

The emulsification curve of PS-g-PA6-Ant2 corresponding to the short time domain shows that the PS dispersed phase domain size does not decrease with the increasing PS-g-PA6-Ant2 concentration until the latter has reached as high as about 1.4 wt%. In other words, below 1.4 wt%, PS-g-PA6-Ant2 cannot play any role in compatibilizing the PS/PA6 (80/20 by mass) blend.

It is interesting to note that the emulsification curves of PS-g-PA6-Ant1 and PS-g-PA6-Ant2 with a pulse of 4.8 g corresponding to the short time domain are above those corresponding to the long time domain, especially for PS-g-

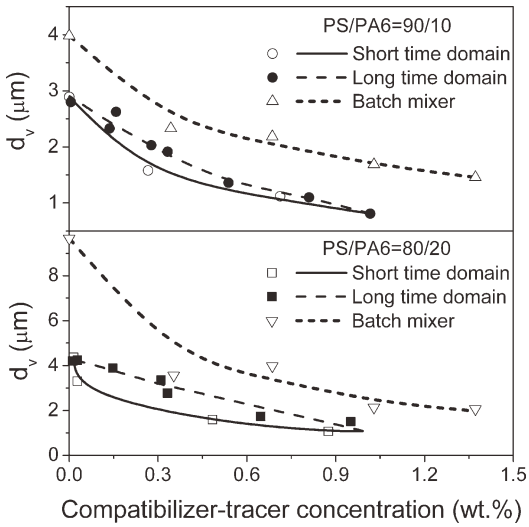

Figure 14. Effect of the type of mixer on the emulsification curve of the PS/PA6 blend.

The data for the short time domain and long time domain are obtained from the twin-screw extruder, whereas those for a batch mixer are obtained from a Haake torque rheometry. Blending conditions in the twin-screw extruder: die width: 5 mm; feed rate: 13 kg/mol; mass of PS-g-PA6-Ant1 pulse: 1.6 g for PS/PA6 (90/10 by mass) and 3.2 g for PS/PA6 (80/20 by mass); screw speed: 100 rpm.

PA6-Ant2. This is exactly the opposite of what is observed for PS-g-PA6-Ant1 with a pulse of 1.6 g (see Figure 6). This is because with a pulse of 4.8 g, it takes more time to disperse the compatibilizer-tracers and drive them to the PS and PA6 interfaces, especially when the concentration of the compatibilizer-tracer is close to above its critical one above which the dispersed domain size does not decrease anymore. This phenomenon may not be easily revealed otherwise if classical approaches are followed to establishing emulsification curves.

The low compatibilizing efficiency of PS-g-PA6-Ant2 is likely related to its high architectural asymmetry. It is expected to have much higher affinity with the PS than the PA6. As a result, thermodynamics does not favor its location at the PS and PA6 interfaces where it is expected to play a role as a compatibilizer. Its peculiar structure may also explain the fact that its emulsification curve corresponding to the short time domain is well above the one corresponding to the long time domain. A longer time might allow better mixing PS-g-PA6-Ant2 in the PS/PA6 blend and bringing it to the PS and PA6 interfaces.

Effect of the type of mixer on the emulsification curve

Figure 14 shows the effect of the type of mixer on the emulsification curve[7,13]. Irrespective of the PS/PA6 mass ratio, the emulsification curves obtained from the twin-screw extruder are significantly below those obtained from the batch mixer of the type Haake rheometer, indicating that the twin-screw extruder has a much higher mixing capacity than the batch mixer.

In summary, the above results show that the concept of the compatibilizer-tracer developed in this article offers a very simple, convenient, and reliable way to construct emulsification curves, selecting most appropriate compatibilizers under given blending conditions. It also allows scaling up and optimizing blending processes, which would otherwise be very difficult or impossible using the classical approaches.

Conclusions

This article reports on a relatively thorough piece of work on the concept of the compatibilizer-tracer and its high application potentials. A compatibilizer-tracer is a compatibilizer such as block or graft copolymer in which a tracer moiety such as a fluorescent label is incorporated. Transient experiments allow using very small amounts of compatibilizer-tracer to obtain emulsification curves, namely, the evolution of the dispersed phase domain size as a function of the compatibilizer-tracer concentration. As such, the concept of compatibilizer-tracer makes it possible for constructing the emulsification curves, selecting most appropriate compatibilizers under real industrial polymer-blending conditions as well as scaling up and optimizing blending processes. It is expected that this concept will trigger new interests in studying or revisiting some of the fundamental issues of polymer blends and blending processes.

Acknowledgments

The authors thank the National Natural Science Foundation of China (grant numbers 50390097 and 20310285), the Ministry of Science and Technology of China through an international cooperation program (grant number 2001CB711203), and the State Key Laboratory of Chemical Engineering (number SKL-ChE-08D03) for the financial support.

Literature Cited

1. Hu GH, Kadri I. Modeling reactive blending: an experimental approach. *J Polym Sci Part B: Phys Ed*. 1998;36:2153–2163.
2. Ryan AJ. Polymer science: designer polymer blends. *Nat Mater*. 2002;1:8–10.
3. Matos M, Favis BD, Lomellini P. Interfacial modification of polymer blends—the emulsification curve: 1. Influence of molecular weight and chemical composition of the interfacial modifier. *Polymer*. 1995;36:3899–3907.
4. Cigana P, Favis BD. The relative efficacy of diblock and triblock copolymers for a polystyrene/ethylene-propylene rubber interface. *Polymer*. 1998;39:3373–3378.
5. Chio WM, Park OO, Lim JG. Effect of diblock copolymers on morphology and mechanical properties for syndiotactic polystyrene/ethylene–propylene copolymer blends. *J Appl Polym Sci*. 2004;91:3618–3626.
6. Harrats C, Fayt R, Jérôme R. Effect of block copolymers of various molecular architecture on the phase morphology and tensile properties of LDPE rich (LDPE/PS) blends. *Polymer*. 2002;43:863–873.
7. Zhang CL, Feng LF, Gu XP, Hoppe S, Hu GH. Efficiency of graft copolymers as compatibilizers for immiscible polymer blends. *Polymer*. 2007;48:5940–5949.
8. Zhang CL, Feng LF, Gu XP, Hoppe S, Hu GH. Blend composition dependence of the compatibilizing efficiency of graft copolymers for immiscible polymer blends. *Polym Eng Sci*. 2010;50:2243–2251.
9. Nauman EB, Buffham BA. *Mixing in continuous flow system*. New York: Wiley, 1983.
10. Chen LQ, Pan ZQ, HU GH. Residence time distribution in screw extruders. *AIChE J*. 1993;9:1455–1464.
11. Chen LQ, HU GH. Application of a statistical theory to residence time distribution. *AIChE J*. 1993;39:1558–1562.
12. Chen, L, Hu GH, Lindt JT. Residence time distribution in non-intermeshing counter-rotating twin screw extruders. *Polym Eng Sci*. 1995,35:598–603.
13. Zhang CL, Feng LF, Hoppe S, Hu GH. Residence time distribution: an old concept in chemical engineering and a new application in polymer processing. *AIChE J*. 2009;55:279–283.
14. Zhang CL, Feng LF, Gu XP, Hoppe S, Hu GH. Tracer-compatibilizer: synthesis and applications in polymer blending processes. *Polym Eng Sci*. In press.
15. Zhang CL, Feng LF, Gu XP, Hoppe S, Hu GH. Determination of the molar mass of polyamide block/graft copolymers by size-exclusion chromatography at room temperature. *Polym Test*. 2007;26:793–802.
16. Zhang CL, Feng LF, Hoppe S, Hu GH. Grafting of polyamide 6 by the anionic polymerization of ε-caprolactam from an isocyanate bearing polystyrene backbone. *J Polym Sci Part A: Polym Chem*. 2008;46:4766–4776.
17. Hu GH, Kadri I. Preparation of macromolecular tracers and their use for studying the residence time distribution of polymeric systems. *Polym Eng Sci*. 1999;39:299–311.
18. Hu GH, Kadri I. On-line measurement of the residence time distribution in screw extruders. *Polym Eng Sci*. 1999;39:930–939.
19. Zhang XM, Xu ZB, Feng LF, Song XB, Hu GH. Assessing local residence time distributions in screw extruders through a new in-line measurement instrument. *Polym Eng Sci*. 2006;46:510–519.
20. Zhang XM, Feng LF, Hoppe S, Hu GH. Local residence time, residence revolution, and residence volume distributions in twin-screw extruders. *Polym Eng Sci*. 2008;48:19–28.
21. Feng LF, Hu GH. Reaction kinetics at polymer-polymer interfaces under flow. *AIChE J*. 2004;50:2604–2614.
22. Hu GH, Li H, Feng LF. A theoretical model for quiescent coalescence in immiscible polymer blends. *AIChE J*. 2002;48:2620–2628.
23. Charoensirisomboon P, Inoue T, Weber M. Pull-out of copolymer in situ-formed during reactive blending: effect of the copolymer architecture. *Polymer*. 2000;41:6907–6912.
24. Zhang CL, Feng LF, Zhao J, Huang H, Hoppe S, Hu GH. Efficiency of graft copolymer at stabilizing co-continuous polymer blends during quiescent annealing. *Polymer*. 2008;49:3462–3469.

Manuscript received Mar. 23, 2011, and revision received Jun. 13, 2011.